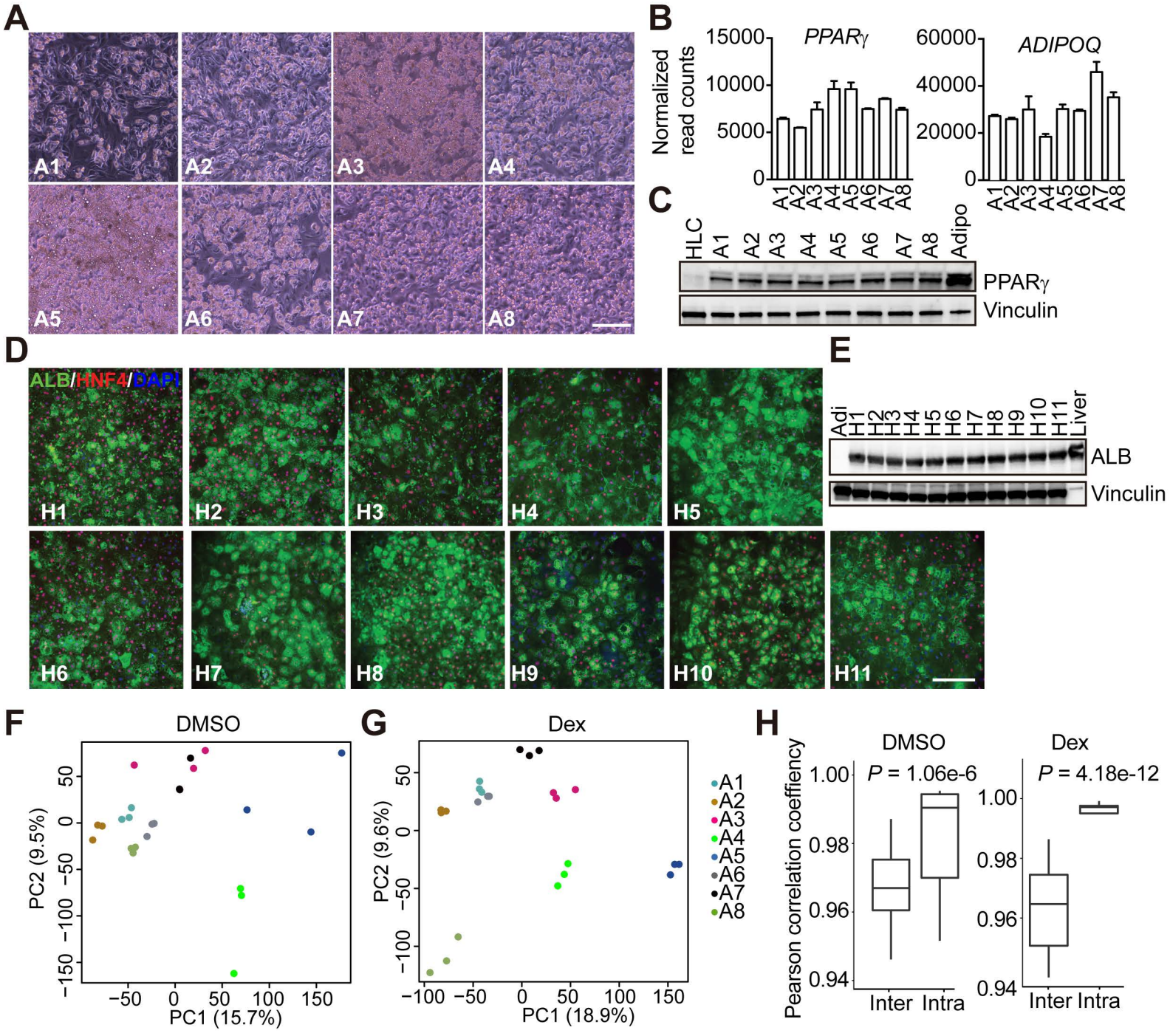

Supplemental Figure 1, related to Figure 1

Figure S1. Derivation and characterization of adipocytes and HLCs from human stem cells, Related to Figure 1.

(A) Representative images of morphology of adipocytes from eight individuals at day 24 (*n* = 2-3). Scale bar, 100 μm.

(B) mRNA expression levels of adipocyte marker genes *PPARγ* and *ADIPOQ* in DMSO-treated adipocytes from eight individuals.

(C) Protein expression level of adipocyte marker gene PPARγ in adipocytes from eight individuals at day 22 (Representative immunoblots (*n* = 2 in total)). HLCs as negative control, primary adipose tissue as positive control.

(D) Representative images of ALB and HNF4 immunostaining of HLCs from eleven individuals at day 20 (*n* = 3-4). Scale bar, 100 μm.

(E) Protein expression level of hepatocyte marker gene ALB in HLCs from eleven individuals at day 20 (Representative immunoblots (*n* = 3 in total)). Adipocytes as negative control, primary liver tissue as positive control.

(F and G) PCA analysis of replicates from adipocytes of eight individuals treated with DMSO (F) or Dex (G) based on all detected genes.

(H) Boxplots show a correlation between biological replicates from the same individual adipocytes (Intra), and between samples from different individuals (Inter) under DMSO or Dex treatment condition. Statistical significance calculated by Wilcoxon rank-sum test. Boxplots show median as a horizontal line, interquartile range as a box.

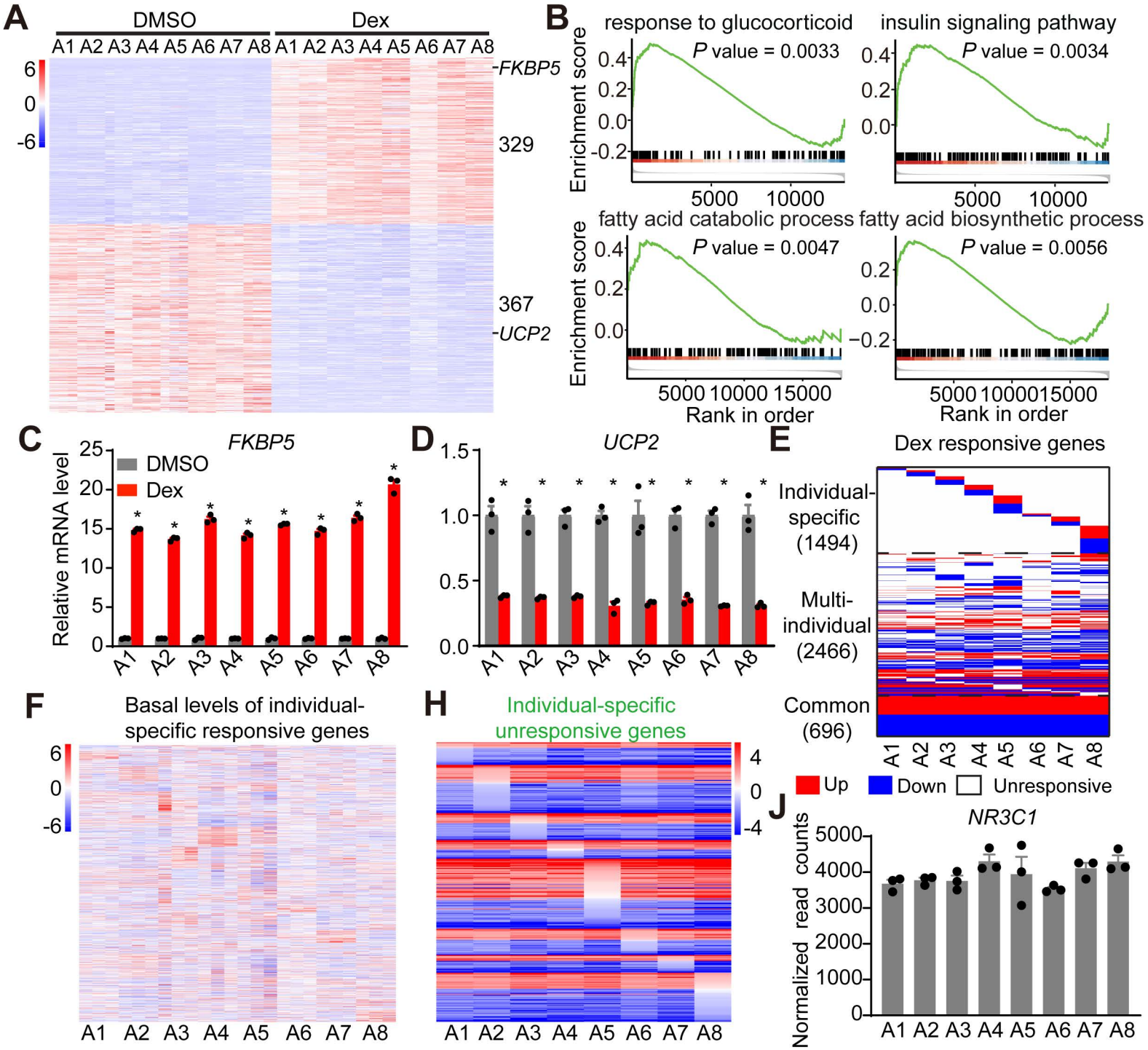

Supplemental Figure 2, related to Figure 1

Figure S2. Individual-derived adipocytes differentially respond to Dex treatment, Related to Figure 1.

(A) Common Dex-responsive genes that are regulated by Dex in adipocytes from all eight individuals. The color bar indicates the scale used to show normalized gene expression values across samples. Differentially expressed genes were identified using DESeq2 with adjusted *P* value < 0.01 and fold change⩾1.5.

(B) GSEA analysis for genes expressed in adipocytes showing the enrichment of key metabolic pathways for Dex-responsive genes. Genes rank by average log2(fold change) in Dex vs DMSO across individuals.

(**C and D**) mRNA expression of common Dex-induced gene *FKBP5* (C) and common Dex-repressed gene *UCP2* (D) in adipocytes from all eight individuals, normalized to DMSO, as measured by RNA-seq.

(E) Heatmap of Dex-responsive genes in only one individual's adipocytes, in multiple individuals' adipocytes and in the adipocytes of all eight individuals. The results of triplicates of each gene are combined for this analysis. The red and blue bars represent up- and down- Dex-responsive genes, while the white bars represent Dex-unresponsive genes.

(F) Heatmap of the basal expression levels of genes that are regulated by Dex in individual-specific manner. The color bar indicates normalized expression value.

(G) Proportion of individual-specific Dex-responsive genes in adipocytes from eight individuals.

(**H**) Heatmap of individual-specific unresponsive genes that are not significantly regulated by Dex in adipocytes from only one individual. The color bar indicates log2(fold change) in Dex vs DMSO.

(I) Proportion of individual-specific Dex-unresponsive genes in adipocytes from eight individuals.

(J) *NR3C1* expression level in adipocytes from eight individuals.

**P* < 0.05, by Student's *t*-test (C and D).

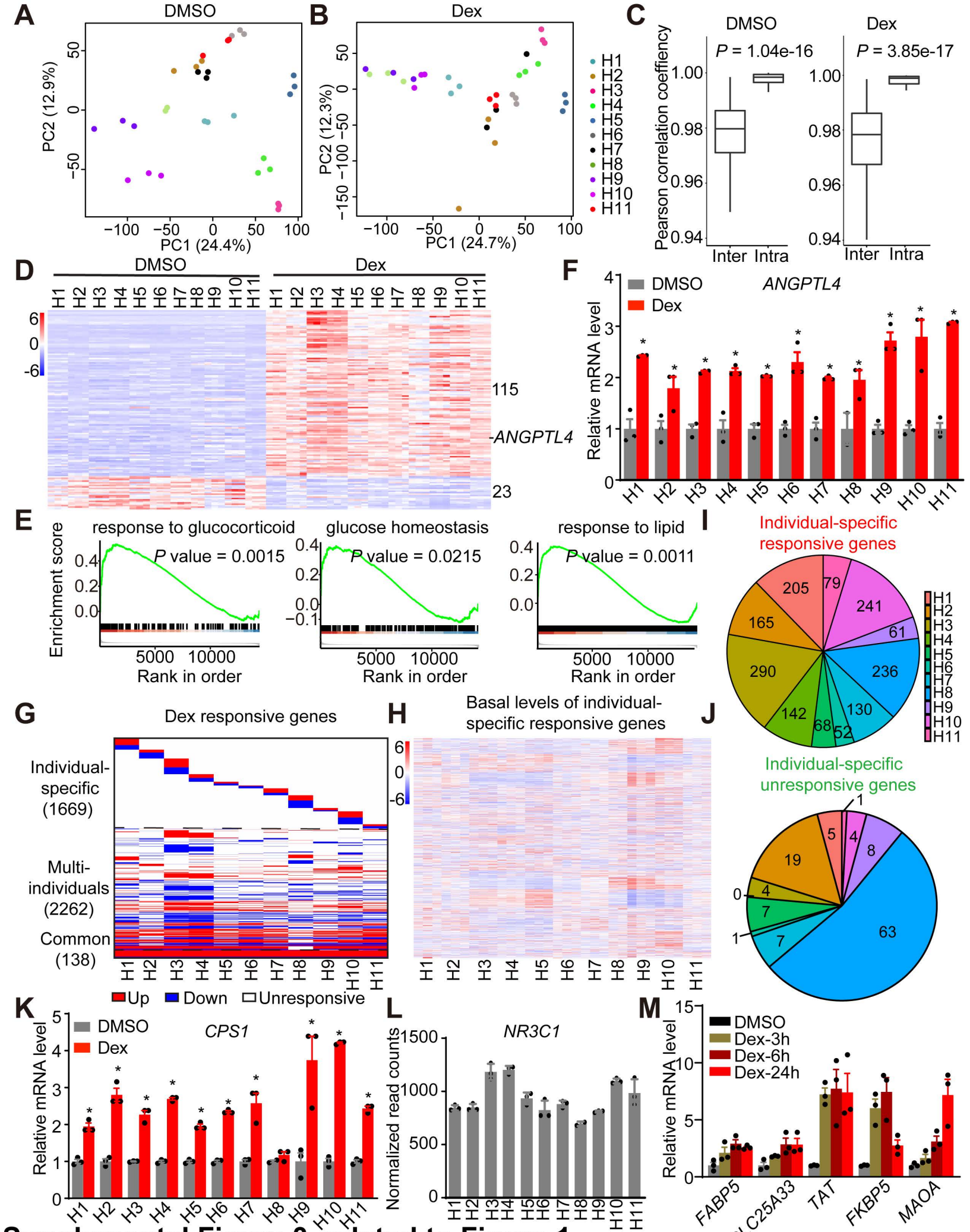

Supplemental Figure 3, related to Figure 1

Figure S3. Individual-derived HLCs differentially respond to Dex treatment, Related to Figure 1.

(A and B) PCA analysis of replicates from HLCs of eleven individuals treated with DMSO (A) or Dex (B).

(C) Boxplots show correlation between biological replicates from the same individual HLCs (Intra), and between samples from different individual (Inter) under DMSO or Dex treatment condition. Statistical significance calculated by Wilcoxon rank-sum test.

(D) Common Dex-responsive genes that are regulated by Dex in HLCs from all eleven individuals. The color bar indicates the scale used to show normalized gene expression values across samples. Differentially expressed genes were identified using DESeq2 with adjusted *P* value < 0.01 and fold change⩾1.5.

(E) GSEA analysis for genes expressed in HLCs showing the enrichment of key metabolic pathways for Dex-responsive genes. Genes were ranked by average log2(fold change) in Dex vs DMSO across individuals.

(**F**) mRNA expression level of common Dex-induced gene *ANGPTL4* in HLCs from all eleven individuals, normalized to DMSO, as measured by RNA-seq.

(G) Heatmap of Dex-responsive genes in only one individual's HLCs, in multiple individuals' HLCs and in the HLCs of all eleven individuals. The results of triplicates of each gene are combined for this analysis. The red and blue bars represent up- and down-Dex-responsive genes, while the white bars represent Dex-unresponsive genes.

(H) Heatmap of the basal expression levels of genes that are regulated by Dex in individual-specific manner. The color bar indicates normalized expression value.

(I and J) Proportion of individual-specific Dex-responsive genes (I) and individual-specific Dex-unresponsive genes (J) in HLCs from eleven individuals.

(**K**) mRNA expression level of H8-specific Dex-unresponsive gene *CPS1* in HLCs from all eleven individuals, normalized to DMSO, as measured by RNA-seq.

(L) *NR3C1* expression level in HLCs from eleven individuals.

(M) mRNA expression levels of GR target genes in HLCs treated with Dex for different time, normalized to HPRT; DMSO was set to 1, as measured by qRT-PCR.

**P* < 0.05, by Student's *t*-test (F and K).

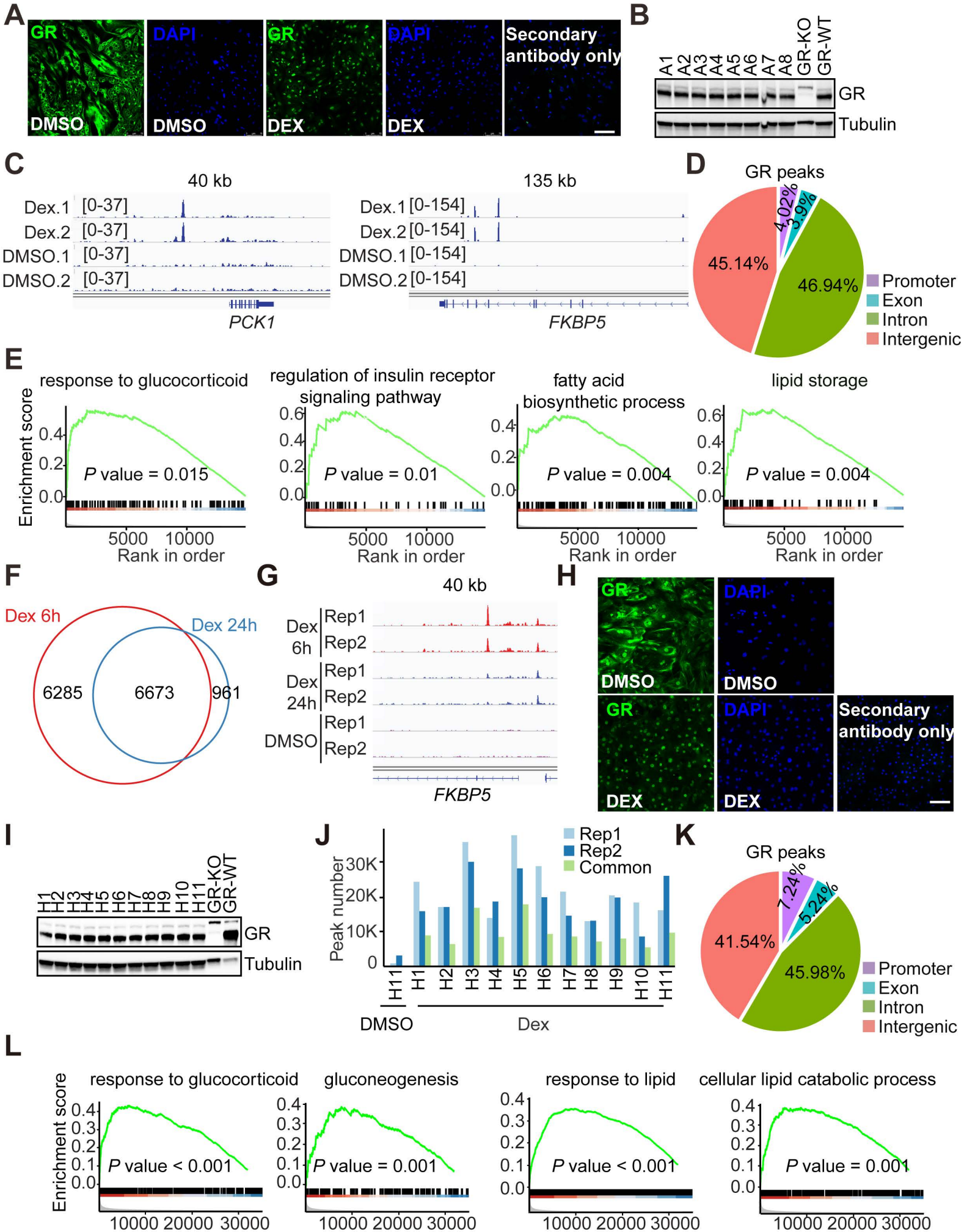

Supplemental Figure 4, related to Figure 2

Figure S4. Cistromes of GR induced by Dex in adipocytes and HLCs, Related to Figure 2.

(A) Representative images of GR immunostaining of adipocytes treated with DMSO or Dex (*n* = 3-4). Scale bar, 100 μm.

(B) Protein expression level of GR in adipocytes from eight individuals treated with Dex (Representative immunoblots (*n* = 2 in total)). GR knockout Hela cell lysates as negative control.

(C) Visualization of the GR binding sites near two classical GR target genes *PCK1* and *FKBP5* in individual H5 adipocytes treated with DMSO or Dex.

(**D**) The distribution of GR binding sites in adipocytes in human genome.

(E) GSEA analysis for the nearest genes of GR bindings in adipocytes showing the enrichment of key metabolic pathways. Genes were ranked by the average intensities of their counterpart peaks across individuals.

(F) Venn diagram demonstrating the GR peak numbers in H11 HLCs treated with Dex for 6hrs or 24hrs.

(G) Visualization of the GR binding sites near the classical GR target gene *FKBP5* in individual H11 HLCs treated with Dex for different time.

(H) Representative images of GR immunostaining of HLCs treated with DMSO or Dex (*n* = 3-4). Scale bar, 100 μm.

(I) Protein expression level of GR in HLCs from eleven individuals treated with Dex (Representative immunoblots (*n* = 3 in total)). GR knockout Hela cell lysates as negative control.

(**J**) GR peak numbers of biological replicates from HLCs treated with DMSO or Dex.

(K) The distribution of GR binding sites in HLCs in human genome.

(L) GSEA analysis for the nearest genes of GR bindings in HLCs showing the enrichment of key metabolic pathways. Genes were ranked by the average intensities of their counterpart peaks across individuals.

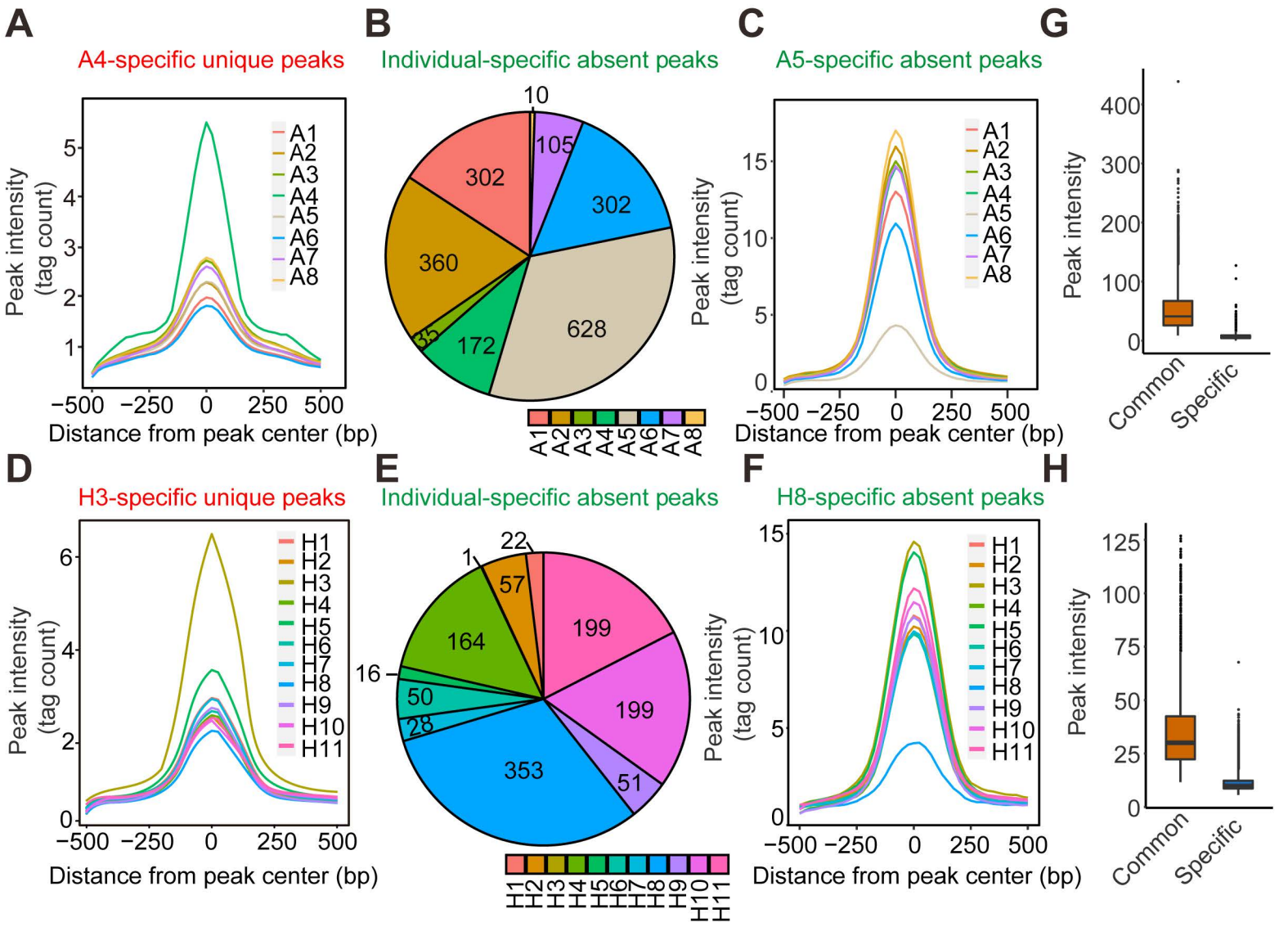

Supplemental Figure 5, related to Figure 2

Figure S5. GR genomic binding shows individual-specific pattern in adipocytes and HLCs, Related to Figure 2.

(A) For A4-specific unique peaks in adipocytes, the average binding profiles are shown in 1 kb windows across individuals.

(B) Proportion of individual-specific absent peaks that are not specifically detected in adipocytes from only one individual.

(C) For A5-specific absent peaks in adipocytes, the average binding profiles are shown in 1 kb windows across individuals.

(D) For H3-specific unique peaks in HLCs, the average binding profiles are shown in 1 kb windows across individuals.

(E) Proportion of individual-specific absent peaks that are not specifically detected in HLCs from only one individual.

(F) For H8-specific absent peaks in HLCs, the average binding profiles are shown in 1 kb windows across individuals.

(G and H) The peak intensities of common GR peaks and individual-specific GR peaks in adipocytes (G) and HLCs (H).

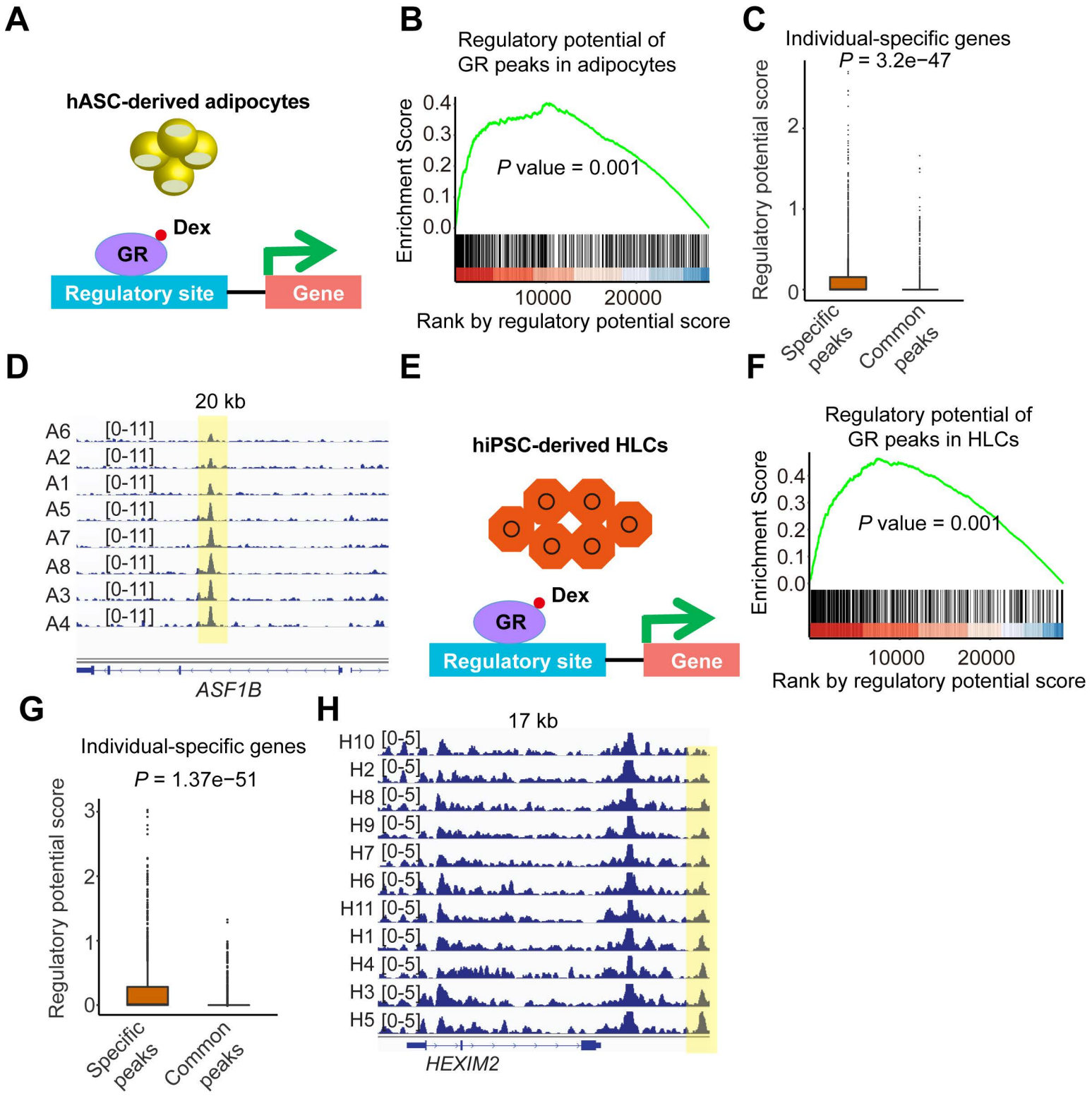

Supplemental Figure 6, related to Figure 3

Figure S6. Individual-specific GR genomic binding and Dex responses, Related to Figure 3.

(A and E) Diagram depicting Dex-induced GR function in adipocytes (A) and HLCs (E).

(B and F) Regulatory potential of GR peaks in adipocytes (B) and HLCs (F). Regulatory potential score was calculated for each gene based on the GR bindings using the regulatory potential model defined by Wang et al., following by the GSEA analysis for all expressed genes ranking by the regulatory potential scores. The black bars in the middle represent Dex-responsive genes.

(C and G) Individual-specific responsive genes are more likely regulated by individual-specific GR binding sites comparing to common GR binding sites in adipocytes (C) and HLCs (G). Regulatory potential score was calculated for each gene based on the near specific GR peaks (or common GR peaks) using the regulatory potential model defined by Wang et al. Statistical significance calculated by Student's *t*-test.

(D and H) Visualization of the GR binding sites near *ASF1B* in all individual adipocytes (D) and *HEXIM3* in all individual HLCs (H) treated with Dex.

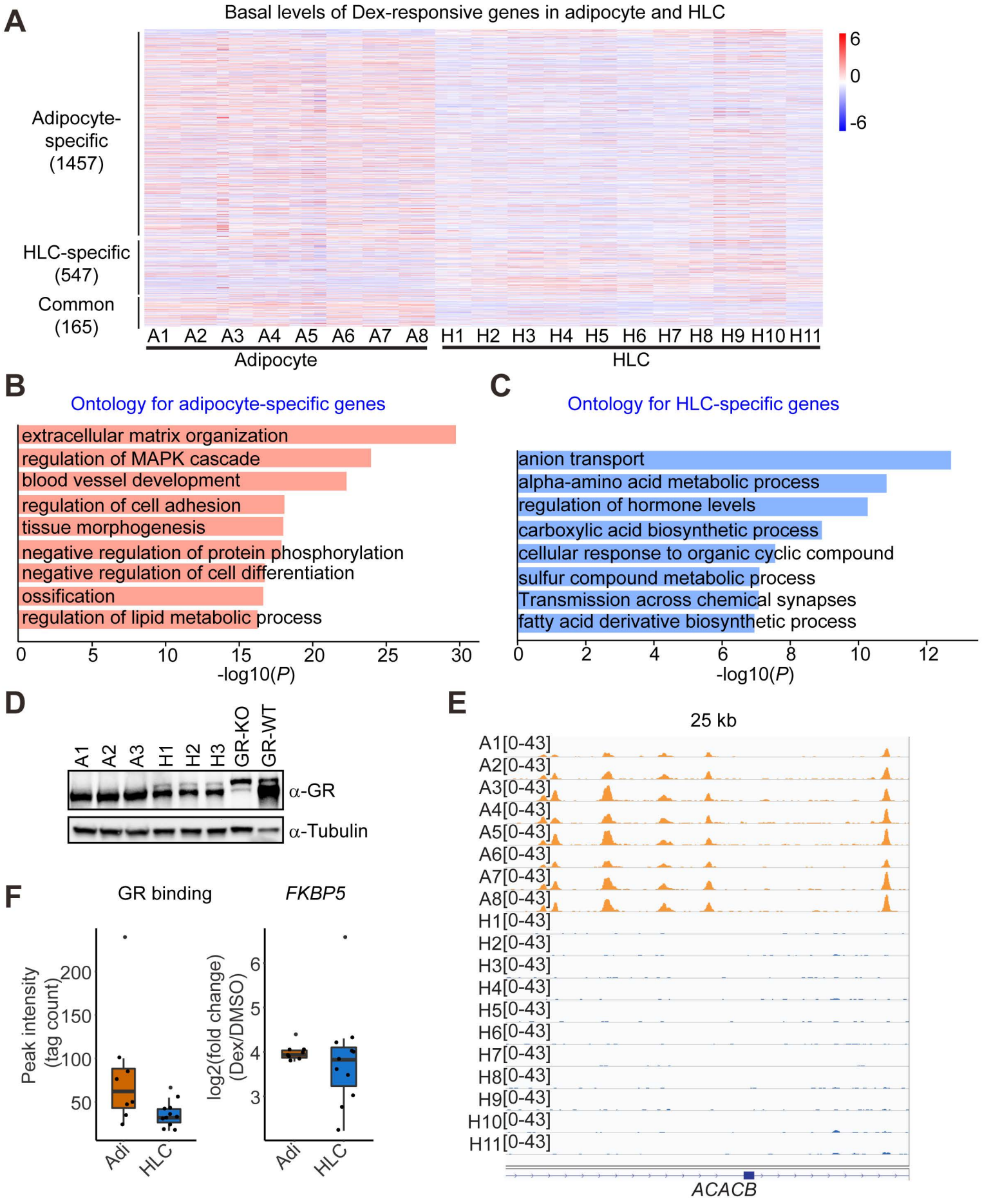

Supplemental Figure 7, related to Figure 4

Figure S7. Cell type-specific GR genomic binding and Dex responses, Related to Figure 4.

(A) The basal expression levels of genes that are uniquely regulated by Dex in adipocytes or HLCs. The color bar indicates the scale used to show normalized gene expression values across samples.

(B and C) Gene ontology for Dex-responsive genes that are detected in at least half of the individual adipocytes (B) or in at least half of the individual HLCs (C).

(**D**) GR protein level in adipocytes and HLCs from three individuals (Representative immunoblots (*n* = 2 in total)). GR knockout Hela cell lysates as negative control.

(**E**) GR ChIP-seq tracks at *ACACB* locus in adipocytes and HLCs.

(**F**) One example gene *FKBP5* that's induced by Dex in both adipocytes and HLCs has nearby GR bindings with strong intensity in both adipocytes and HLCs. Boxplots show median as a horizontal line, interquartile range as a box.

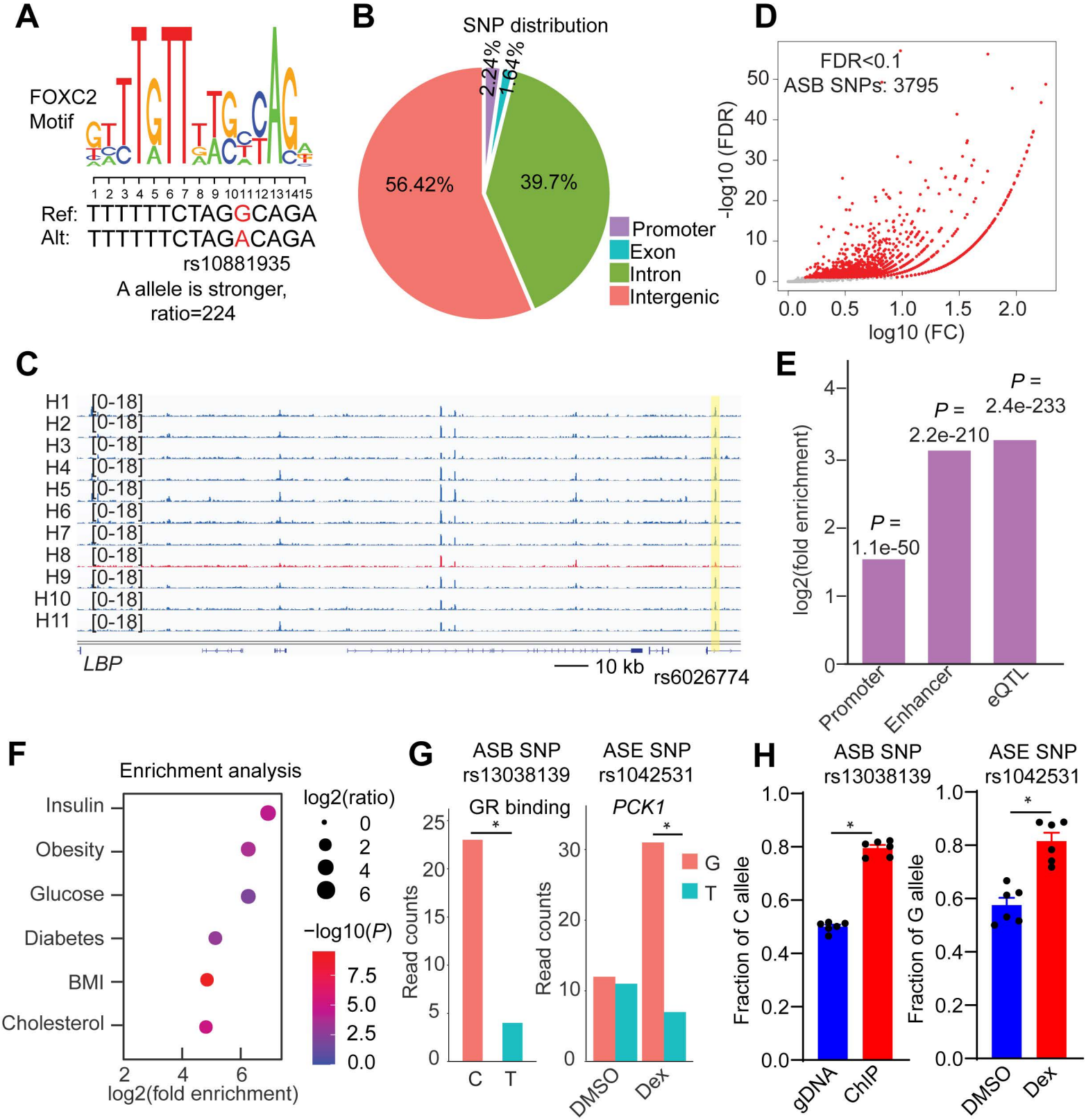

Supplemental Figure 8, related to Figure 5

Figure S8. Genetic variations modulate GR function and Dex responses, Related to Figures 5.

(A) The putative effect of rs10881935 on FOXC2 motif.

(B) The distribution of SNPs from Infinium Human CoreExome-24 BeadChip in human genome.

(C) Visualization of a H8-specific absent peak region (yellow box) at *LBP* locus across individuals.

(**D**) Scatter plot showing the SNPs that significantly affect GR binding in allele-specific manner. Red dots represent allele-specific binding (ASB) SNPs. FDR was adjusted from *P* values calculated using Exact Binomial Test.

(E) Enrichment of SNPs that determine allele-specific GR binding in promoter, enhancer and eQTL from liver in GTEx. Statistical significance calculated by hypergeometric test.

(F) Enrichment of SNPs that determine allele-specific GR binding for metabolic traits-associated SNPs from GWAS Catalog. Statistical significance calculated by hypergeometric test.

(**G**) Read counts of reference and alternative alleles at ASB SNP rs13038139 and allele-specific expression (ASE) SNP rs1042531 showed imbalanced GR binding (left) and allele-selectively induced *PCK1* (right) by Dex. *FDR < 0.05 (Exact Binomial Test).

(H) GR ChIP-qPCR products and cDNA of HLCs treated with DMSO or Dex from two heterozygous individuals (n=3) were assayed for imbalance at SNPs using a SNaPshot assay, with gDNA and cDNA from DMSO-treated HLCs showing no imbalance. Data are expressed as mean ± SEM. *P < 0.05 (Student's t-test).

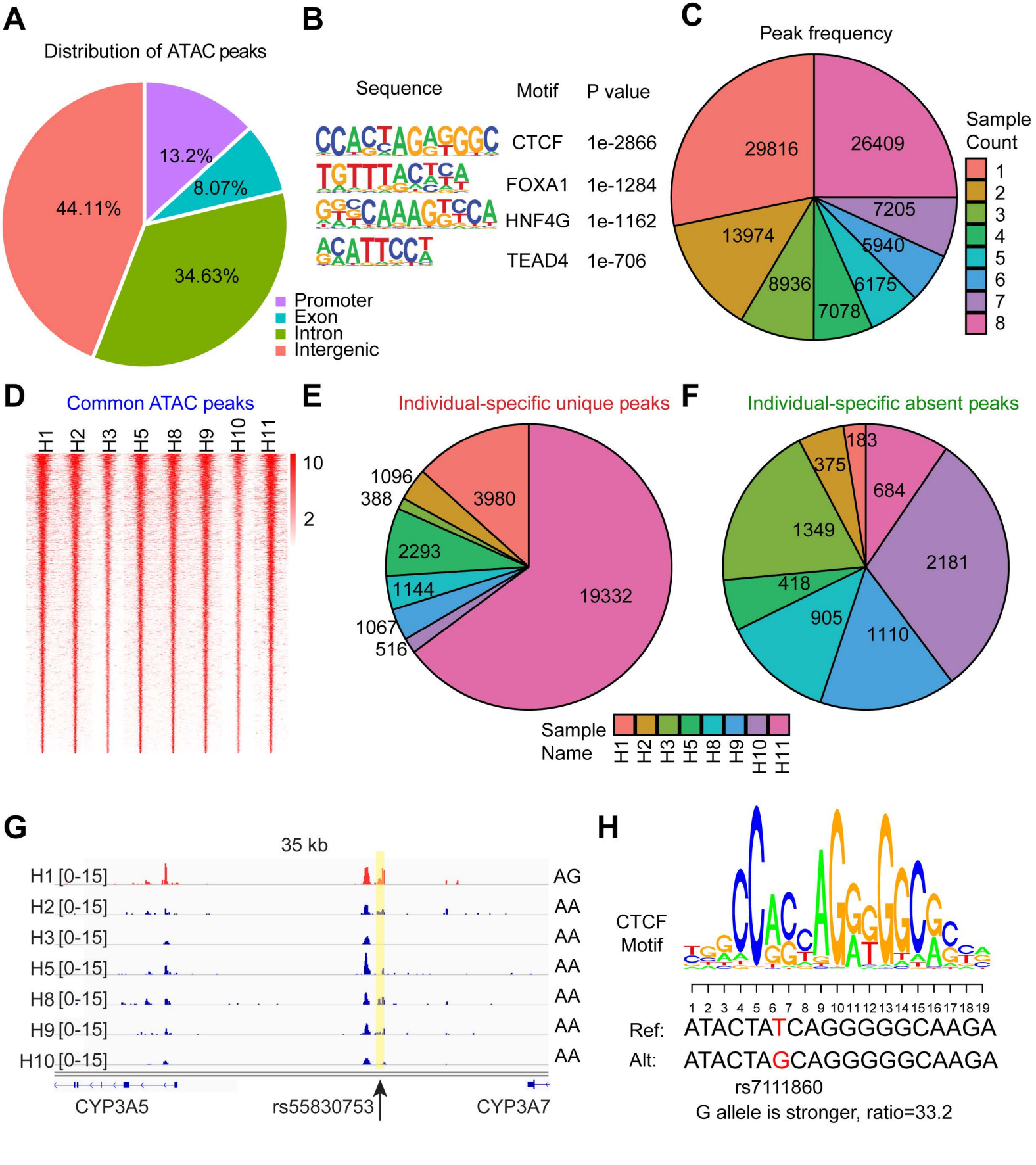

Supplemental Figure 9, related to Figure 6

Figure S9. ATAC-seq and ChIA-PET analysis, Related to Figures 6.

(A) The distribution of ATAC peaks of HLCs in human genome.

(B) Consensus motif logos for the top-scoring motif families found in ATAC peaks in HLCs treated with Dex.

(C) The number of ATAC peaks detected in HLCs from one individual to eight individuals.

(D) Heatmap of common ATAC peaks that are detected similarly in HLCs from eight individuals. The color bar indicates the scale of normalized tag counts.

(E) Proportion of individual-specific ATAC peaks that are specifically detected in HLCs from only one individual.

(F) Proportion of individual-specific absent ATAC peaks that are not specifically detected in HLCs from only one individual.

(G) Visualization of a H1-specific unique ATAC peak region (yellow box) at *CYP3A5/CYP3A7* locus across individuals. Black arrow indicates the position of rs55830753.

(H) The putative effect of rs7111860 on CTCF motif.

A

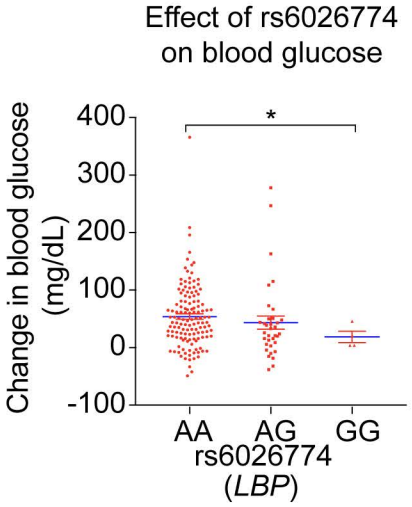

B

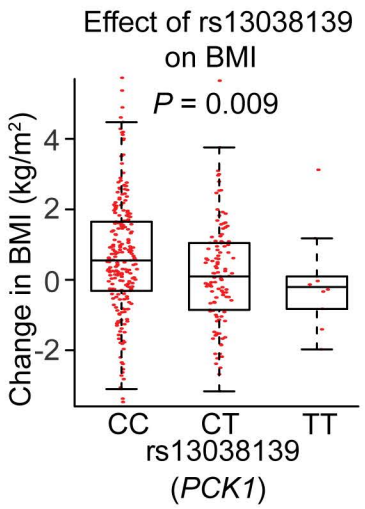

C

rsid	phenotype	snpid	hazard ratio (odds ratio for MRD)	ci95.low	ci95.high	*P* value
rs13038139	any_relapse	20:56161598_T	1.5	0.88	2.57	0.138
	mrd_d19	20:56161598_T	1.08	0.79	1.48	0.637
	mrd_d46	20:56161598_T	1.04	0.68	1.59	0.851
rs55830753	any_relapse	7:99292222_G	1.28	0.69	2.36	0.43
	mrd_d19	7:99292222_G	0.96	0.64	1.43	0.829
	mrd_d46	7:99292222_G	0.84	0.47	1.5	0.55
rs10980797	any_relapse	9:113912553_G	1.15	0.75	1.77	0.513
	mrd_d19	9:113912553_G	1.03	0.8	1.32	0.823
	mrd_d46	9:113912553_G	0.97	0.7	1.35	0.859
rs10881935	any_relapse	10:93397701_G	0.48	0.26	0.88	0.017
	mrd_d19	10:93397701_G	0.86	0.66	1.12	0.275
	mrd_d46	10:93397701_G	0.79	0.55	1.15	0.218
rs2060982	any_relapse	11:68612927_A	1.28	0.79	2.08	0.309
	mrd_d19	11:68612927_A	1.05	0.81	1.37	0.693
	mrd_d46	11:68612927_A	1.09	0.77	1.55	0.633

Figure S10. Clinical relevance of the identified SNPs, Related to Figures 7.

(A) The change of maximal glucose level after GC treatment in individuals carrying different genotypes at rs6026774. Data are expressed as mean ± SEM. *P < 0.05 (Student's t test).

(B) The change of BMI after Dex treatment in ALL individuals carrying different genotypes at rs13038139. Boxplots show median as a horizontal line, interquartile range as a box. P value was calculated by multiple logistic regression analysis.

(C) The association between the identified SNPs and treatment outcome ("any relapses") and early treatment response (minimal residual disease during [mrd_day19] or at the end of [mrd_day46] of remission/induction therapy.

Table S1. Primers used in this study, Related to STAR Methods.

Primer for RT-qPCR		
Primers	**Forward (5'-3')**	**Reverse (5'-3')**
LBP	CTACAGGGCTCCTTTGATGTCA	CACGTCAGCGATGTCACTG
HPRT	TGACACTGGCAAAACAATGCA	GGTCCTTTTCACCAGCAAGCT
FABP5	GCTGATGGCAGAAAAACTCAGA	CCTGATGCTGAACCAATGCA
SLC25A33	TGTGCTCGTTACGTTTACCAG	AGTTTCGGAAATTCCAGCATACG
TAT	CTGGACTCGGGCAAATATAATGG	GTCCTTAGCTTCTAGGGGTGC
FKBP5	CTCCCTAAAATTCCCTCGAATGC	CCCTCTCCTTTCCGTTTGGTT
MAOA	GTGGGACCAACCCAAAACAGA	ATATTGAACGAGACGCTCACTG
Primer for ChIP-qPCR		
Primers	**Forward (5'-3')**	**Reverse (5'-3')**
LPAR1	ACCTCACCATTGTATGAATTTTGGA	CACATTTCGCAAACTGTTTTTCACA
FKBP5	TGCAAAACATCACTTAAACTGGA	CCACATTCAGAACAGGGTGT
LBP	TTTGCTCCAGGCTAATGTTC	ACTAAATGACTCACAAGCAAGG
PDK4	TCACTAGGGGAAAGGTCGGG	TAACAGCCAGGAGACTCACG
INS2	GCCCACCCTCTGATGTATCT	AAAGTGACCAGCTCCCTGTG
Primer for SNaPshot		
Primers	**Forward (5'-3')**	**Reverse (5'-3')**
PCK1-ASB PCR	CACACGCTGCAAAGTCCAG	TGTTTCGGAGTCAGGACATCAC
PCK1-ASB SNaPshot	GGCCTGTGAAGCGAGCAACAA	
PCK1-ASE PCR	CAGTAGGAGCAAGAGAGGGC	GGCATGCTAAGATTTCCCTTC
PCK1-ASE SNaPshot	CATAATAATCATCACCACACCG	
gBlocks Gene for Luciferase reporter cloning		
rs6026774-A (5'-3')	CCGCTCGAGTAAATTAAACTTATAAAATCAGCTTATAATAATATCACCGTTAC CTCTTTTGTTTATTGAGAAGACATTCCACTGCCAAAGAAAAAAAAAAAAGCGA AAACTACTTCCCTGGAACAAGGTTGGTCTGTTTGCTCCAGGCTAATGTTCTT GTGTATTGGCTCACAAGGTCACTAGGTCAGCTCCCCCAATCCTTTGAGTCTG TTCATCTCACTGGTCCCTTGCTTGTGAGTCAGATCTTCC
rs6026774-G (5'-3')	CCGCTCGAGTAAATTAAACTTATAAAATCAGCTTATAATAATATCACCGTTAC CTCTTTTGTTTATTGAGAAGACATTCCACTGCCAAAGAAAAAAAAAAAAGCGA AAACTACTTCCCTGGAACGAGGTTGGTCTGTTTGCTCCAGGCTAATGTTCTT GTGTATTGGCTCACAAGGTCACTAGGTCAGCTCCCCCAATCCTTTGAGTCTG TTCATCTCACTGGTCCCTTGCTTGTGAGTCAGATCTTCC